Electronic Supplementary Material (ESI) for Inorganic Chemistry Frontiers.

Supporting information for:

Synthesis and characterization of a stable and inert Mn^{II}-based Zn^{II} responsive MRI probe for molecular imaging of glucose stimulated zinc secretion (GSZS)

Richárd Botár,[ab] Enikő Molnár,[a] Zoltán Garda,[a] Enikő Madarasi,[ab] György Trencsényi,[c] János Kiss,[c] Ferenc K. Kálmán[a]* and Gyula Tircsó[a]*

[a] *Department of Physical Chemistry, Faculty of Science and Technology, University of Debrecen, H-4032, Debrecen, Egyetem tér 1., Hungary*

[b] *Doctoral School of Chemistry at the University of Debrecen, H-4032, Debrecen, Egyetem tér 1., Hungary.*

[c] *Division of Nuclear Medicine, Department of Medical Imaging, Faculty of Medicine, University of Debrecen, H-4032, Debrecen, Egyetem tér 1., Hungary*

Table of content

Synthesis of the PC2A-DPA ligand

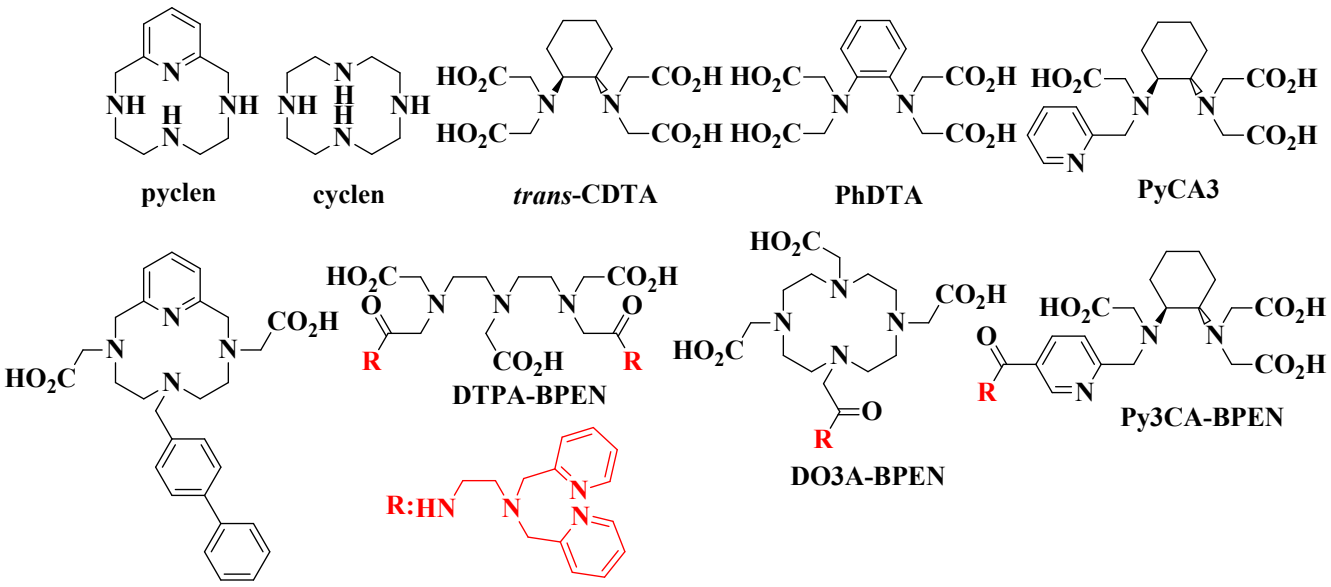

Scheme S1. Structures of the ligands mentioned in the text.

General procedures

Thin layer chromatography (TLC) was conducted on Aluminum sheets (TLC Silica 60 F245) obtained from Merck. The NMR measurements were carried out with Bruker DRX 360 spectrometer using the corresponding deuterated ($CDCl_3$, CD_3CN, D_2O) solvents. ESI-MS spectra were recorded on maXis II UHR ESI-TOF MS (Bruker) mass spectrometer. The synthetic reactions were followed by using a Waters Alliance 2690 HPLC equipped with Waters 996 PDA detector, and a Phenomenex C18(2) 150*4,6 mm 3 micron column. The preparative HPLC separations were done by using preparative HPLC YL9101S degasser, YL9110S pump, YL9120S UV/VIS detector, Phenomenex Luna Prep C18(2) 100A 250x21.20 mm 10 micron 00G-4324-P0 column and Sigma-Aldrich CHROMASOLV® Plus solvents.

Abbreviations:

TREN: tris(2-aminoethyl)amine

HPLC: High Performance Liquid Chromatography

TFA: trifluoroacetic acid

Table S1. Solvent composition used during the preparative HPLC separation (for analytical work).

t (min)	ACN (%)	Water with 0.005 M TFA (%)
0	10	90
10	90	10
11	10	90
13	10	90

Table S2. Solvent composition used during the preparative HPLC separation of the [Mn(PC2A-DPA)] complex used for the *in vivo* experiments.

t (min)	ACN (%)	Water (%)
0	10	90
10	90	10
11	10	90
13	10	90

Details of the synthesis

N,N',N''-(nitrilotris(ethane-2,1-diyl))tris(4-methylbenzenesulfonamide) (3): TREN **(1)** (10.0 g, 68,5 mmol) and NaOH (9.00 g, 226 mmol) were dissolved in 100 mL of bidistilled water, then a solution of tosyl-chloride **(2)** (39.0 g, 206 mmol) in 180 mL diethyl ether was added dropp-wise slowly to this mixture under vigorous stirring. After the evaporation of the ether the white precipitate formed was filtered off and dried under heating lamp until constant weight resulting product **(3)** with 94 % yield. ^{1}H-NMR: (CD_3CN; 360 MHz): δ (ppm) 2.32 (t; 6 H) 2.41 (s; 9 H) 2.75 (q; 6 H) 5.41 (bs; 3 H) 7.10 (d; 6 H) 7.45 (d; 6 H).[1]

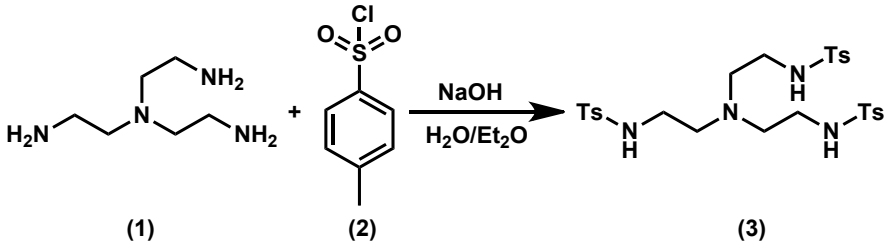

***N*-[2-[3,9-Bis[tosyl]-3,6,9,15-tetraazabicyclo[9.3.1]pentadeca-1(15),11,13-triene-6-il]ethyl]-4-methyphenylsulfamide (5):** Solution of 2,6-chloromethyl pyridine **(4)** (5.78 g, 32.9 mmol) in anhydrous acetonitrile (100 mL) was added dropwise to the mixture of **(3)** (20.0 g, 32.9 mmol) and freshly dried K_2CO_3 (44.4 g, 328 mmol) in anhydrous acetonitrile (400 mL) at 80 °C. The reaction was monitored using analytical HPLC technique. Upon completion of the reaction the solid was filtered off and the

solvent was evaporated under vacuum yielded the product **(5)** 92 %. ^{1}H-NMR: (CD_3CN; 360 MHz): δ (ppm) 2.33 (t; 2 H) 2.43 (9; H) 2.51 (t; 4 H) 3.31 (t; 4 H) 3.62 (t; 2 H) 4.81 (s; 4 H) 7.03 (d; 2 H) 7.41 (d; 2 H) 7.52 (d; 4 H) 7.59 (t; 1 H) 7.68 (d; 2 H) 7.81 (d; 4 H).[2]

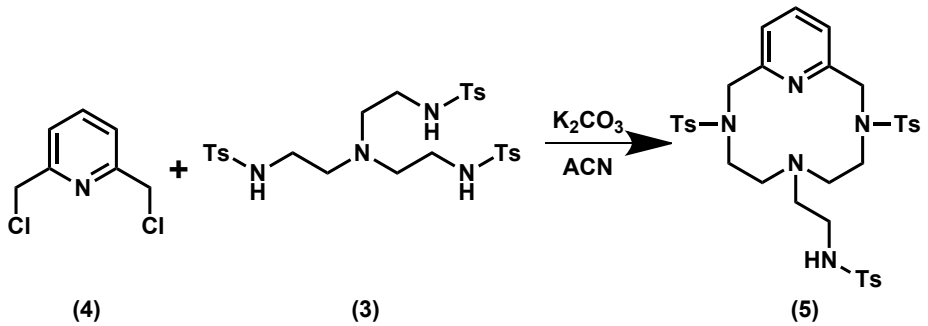

(4) (3) (5)

3,6,9,15-Tetraazabicyclo[9.3.1]pentadeca-1(15),11,13-triene-6-ethaneamine (6) (*6*-PAE): Compound **(5)** (10.7 g, 14.04 mmol) was dissolved in concentrated sulfuric acid (60.0 mL) heated up and kept at 180 °C for 3 min. The reacton mixture was cooled to room temperature and then to 0 °C using water/ice cooling mixture and was added dropvise to ice cold diethyl ether (500 mL). The solvent was decantated and the oily residue was dissolved in bidistilled water (50.0 mL). The pH of the aqueous solution was set at 12 with the use of solid NaOH extracted with chloroform (3X500 mL). The organic phase was separated and was dried with $MgSO_4$, filtered and evaporated under reduced pressure. The yield of the title compound (yellowish oil) is 98%. ^{1}H-NMR: (D_2O; 360 MHz): δ (ppm) 2,83 (m; 4H) 2,92 (m; 2H) 3,19 (m; 6H) 4,54 (s; 4H) 7,36 (d; 3H), 7,85 (t; 2H).[3]

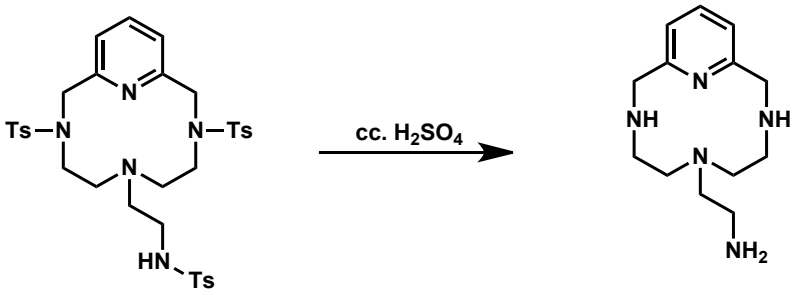

(5) (6)

***N*-(phtalimido)-3, 6,9,15-tetraazabicyclo[9.3.1]pentadeca-1(15),11,13-triene-6-ethaneamine (8):** Phtalic anhydride **(7)** (2.00 mmol, 296 mg) was dissolved in glacial acetic acid and then added to the solution of **(6)** (1.00 g, 4.00 mmol) in glacial acetic acid (10.0 mL). This mixture was treated with microwave (10 min, 120 °C, 50 W). The reaction mixture was cooled, frozen and liophylized yielding the **(8)** as a yellowish oil (Yield of 88%). ^{1}H-NMR: (CD_3CN; 400 MHz): δ (ppm) 2,88 (s; 4H) 2,93 (t; 2H) 3,10 (s; 4H) 3,77 (t; 2H) 4,47 (s; 4H) 7,36 (d; 2H) 7,77 (m; 4H) 7,87 (t; 1H).[4]

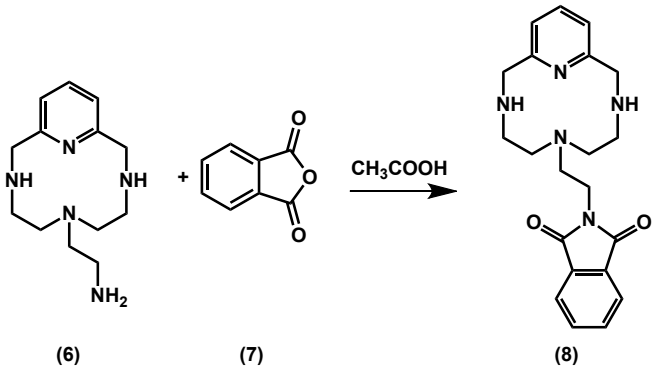

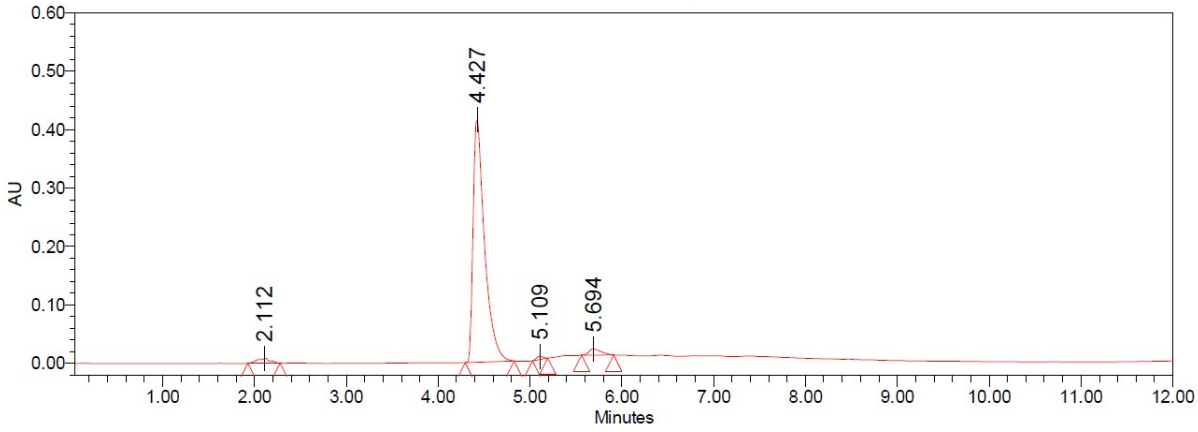

Figure S1. HPLC chromatogram of the product (using the solvent composition as outlined in Table S1, HPLC purity is 94.5%).

Di-*tert*-butyl-6-(2-(1,3-dioxoisoindolinyl)-ethyl)-3,6,9,15-tetraazabiccylo[9.3.1]pentadeca-1(15),11,13-triene-3,9-diacetate (10): Solution of tert-butyl bromoacetate **(9)** (144 µL, 0.98 mmol) in 25.0 mL acetonitrile was added dropwise to the mixture of **(8)** (230 mg, 0.61 mmol) and K_2CO_3 (415 mg, 3.05 mmol) at 60 °C in acetonitrile (50.0 mL). After one hour the mixture was cooled down to room temperature, the solids were filtered off and the solvent was evaporated under vacuum, yielding the title compund as white solid at 52 %. ^{1}H-NMR: ($CDCl_3$; 360 MHz): δ (ppm) 1,46 (s; 18 H) 1,83 (s; 2 H) 2,52 (m; 6 H) 2,88 (s; 2 H) 3,46 (s; 6 H) 3,69 (t; 2 H) 4,01 (d; 2 H) 7,05 (d; 2 H) 7,56 (t; 1 H) 7,69 (dd; 2 H) 7,80 (dd; 2 H); ^{13}C-NMR: ($CDCl_3$; 360 MHz): δ (ppm) 20.91; 34.46; 45.91; 49.46; 50.97; 53.14; 117.57; 121.80; 123.1; 132.01; 134.36; 139.21; 150.26; 168.78; 174.78 ESI-MS: *m/z* $[M+H]^+$.608.347 (theoretical $[M+H]^+$ 608.340).

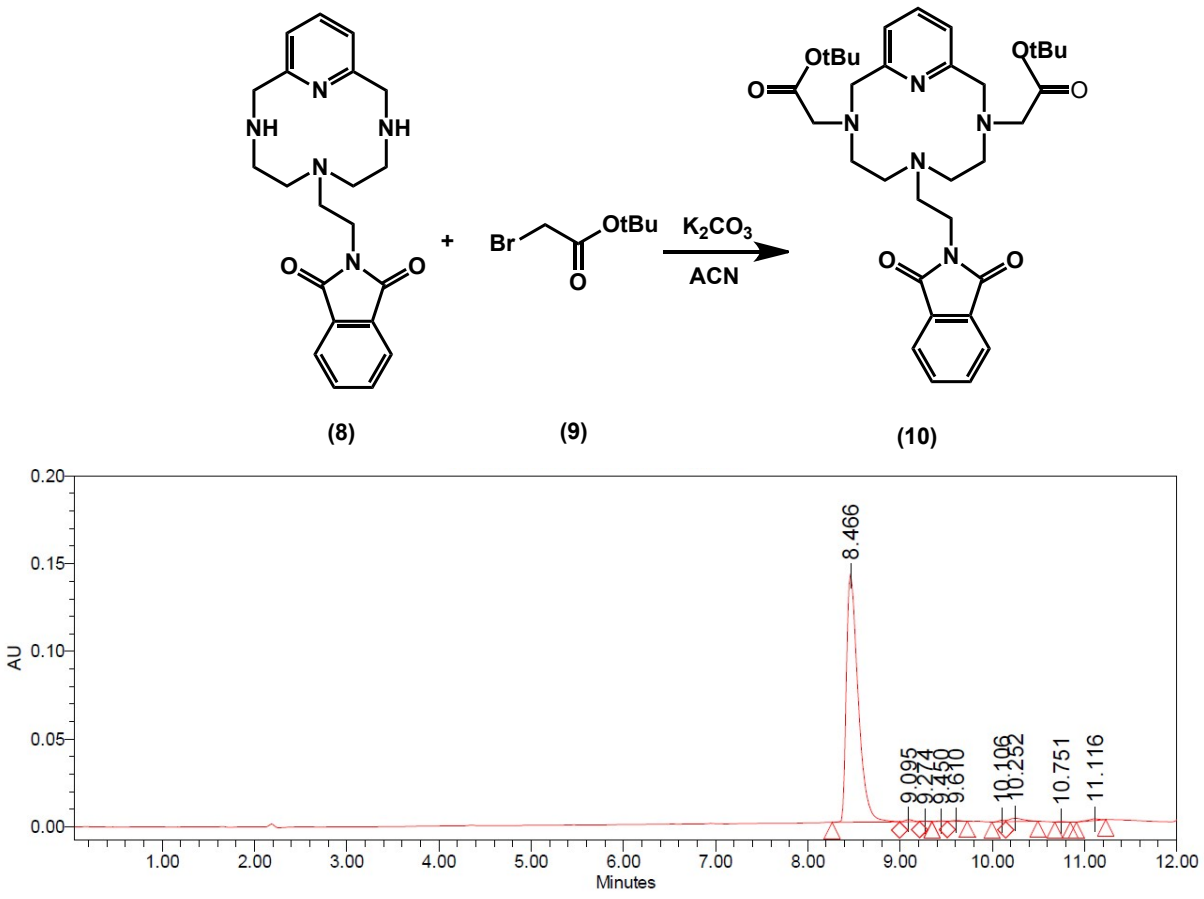

Figure S2. HPLC chromatogram of the product (using the solvent composition as outlined in Table S1, HPLC purity is 96.3%).

Di-*tert*-butyl-6-(2-aminoethyl)-3,6,9,15-tetraazabicyclo[9.3.1]pentadeca-1(15),11,13-triene-3,9-diacetate (11): Hydrazine-hydrate (213 µL, 5.45 mmol) was added to the solution of **(10)** (440 mg, 0.73 mmol) in ethanol (10.0 mL) and the solution was treated with microwave for 60 min at 80 °C, the applied power was 120 W. After cooling the reaction mixture the white precipitate formed was filtered off and the solvent was evaporated under reduced pressure. The title compound was obtained as a white powder (yield: 42%). ^{1}H-NMR: (CD_3CN; 360 MHz): δ (ppm) 1,47 (s; 18H) 2,45 (s; 8H) 2,70 (s; 3H) 2,85 (s; 3H) 3,43 (s; 4H) 3,91 (s; 4H) 7,11 (d; 2H) 7,65 (t; 1H).[5]

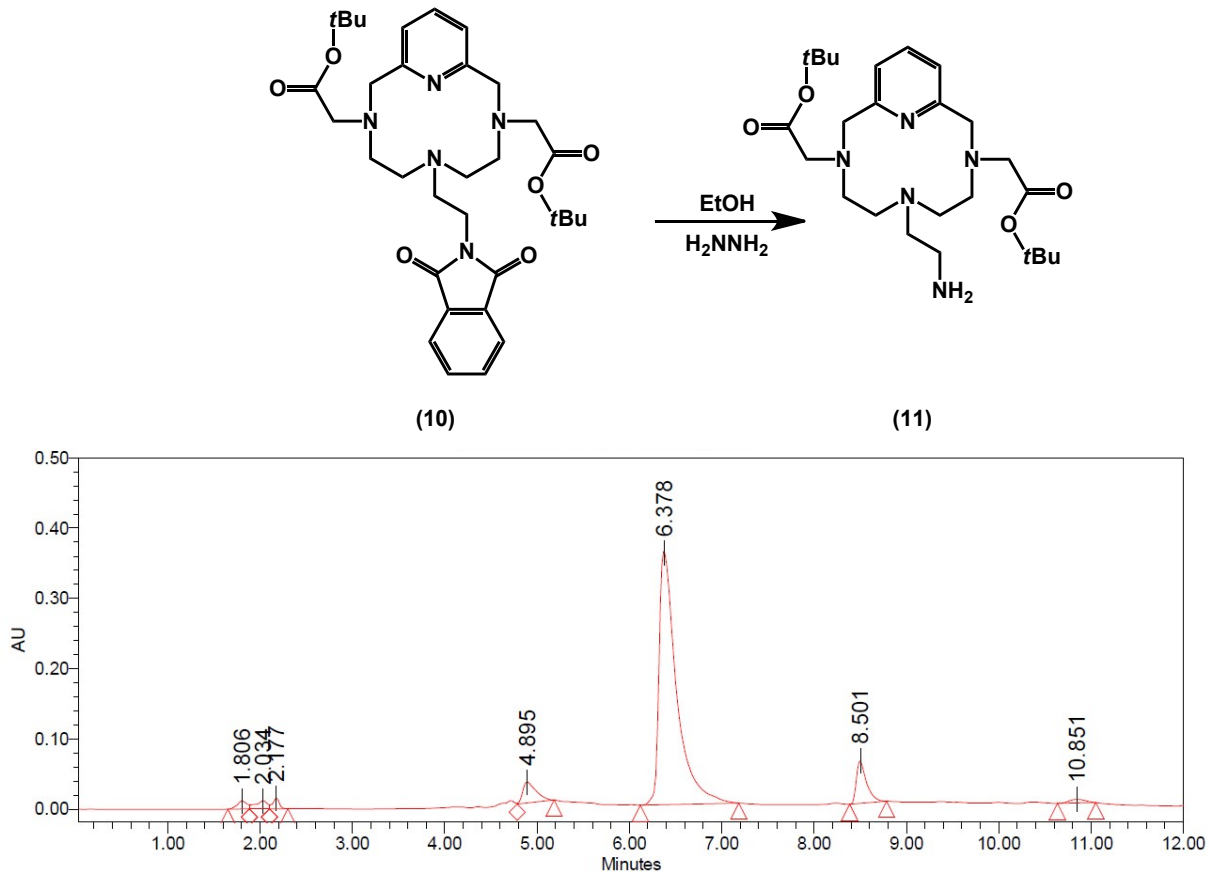

Figure S3. HPLC chromatogram of the product (using the solvent composition as outlined in Table S1, HPLC purity is 81.5%).

Di-*tert*-butyl-6-(*N*-bis(2-pyridinylmethyl)-2-aminoethyl)-3,6,9,15-tetraazabicyclo[9.3.1]pentadeca-1(15),11,13-triene-3,9-diacetate (13): Solution of 2-(chloromethyl)pyridine hydrochloride **(12)** (139 mg, 0.86 mmol) in anhydrous acetonitrile (5.00 mL) was added drop-wise to the mixture of **(11)** (93.0 mg, 0.19 mmol), K_2CO_3 (160 mg, 1.17 mmol) and NaI (5.70 mg, 0.038 mmol) in anhydrous acetonitrile (25.0 mL) at room temperature under stirring. The progress of the reaction was followed by analytical HPLC technique. When the signal of the starting material disappeared the solid present in the reaction mixture was filtered off and the solvent was evaporated under vacuum yielded the **(13)** at 72 %. ^{1}H-NMR: (CD_3CN; 360 MHz): δ (ppm) 1,41 (s; 18H) 2,81 (s; 2H) 2,94 (s; 2H) 3,11 (s; 8H) 3,44 (s; 4H) 4,00 (s; 4H) 4,26 (s; 4H) 7,22 (d; 2H) 7,78 (t; 1H) 7,87 (m; 4H) 8,39 (t; 2H) 8,80 (d; 4H) ESI-MS: *m/z* $[M+H]^+$ 660.423 (theoretical $[M+H]^+$ 660.424).

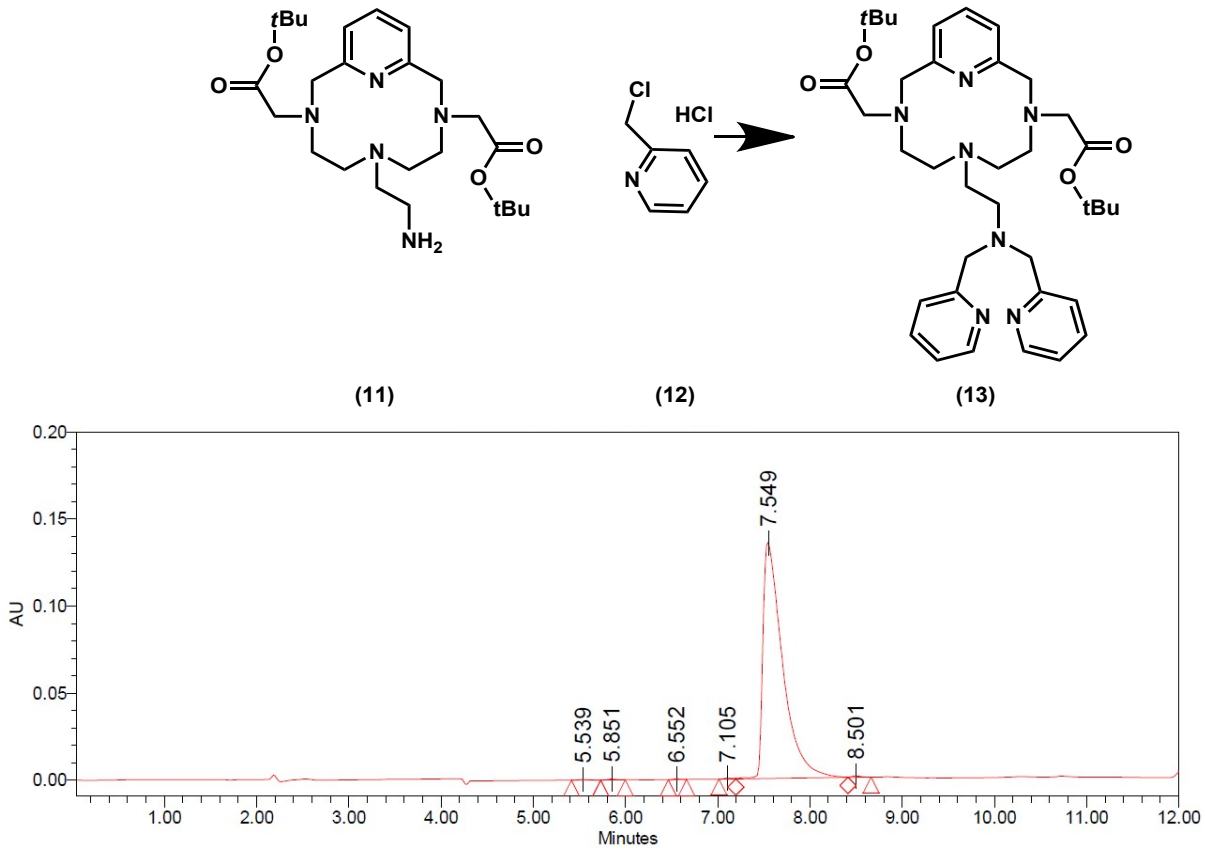

Figure S4. HPLC chromatogram of the product (using the solvent composition as outlined in Table S1, HPLC purity is 99.2%).

6-(*N*-bis(2-pyridinylmethyl)-2-aminoethyl)-3,6,9,15-tetraazabicyclo[9.3.1]pentadeca-1(15),11,13-triene-3,9-diacetic acid (14): NaOH (14.2 mg, 0.36 mmol) was added to the solution of **(13)** (59.0 mg, 0.089 mmol) in ethanol (10.0 mL) and the reaction mixture was heated to reflux and kept at this temperature for 6 hours. The reaction mixture was cooled down and the crude product was purified using preparative HPLC technique mentioned above. The solvent was lyophilized leaving the title compound as a yellowish oil (yield: 98%). ^{1}H-NMR: (D_2O; pH=1,81; 360 MHz): δ (ppm) 3,22 (d; 6H) 3,4 (s; 4H) 3,54 (s; 2H) 4,02 (s; 4H) 4,38 (s; 4H) 4,64 (s; 4H) 7,73 (d; 2H) 7,98 (t; 2H) 8,10 (d; 2H) 8,32 (t; 1H) 8,55 (t; 2H) 8,75 (d; 2H) ^{13}C-NMR: ($CDCl_3$; DRX-360 MHz): δ (ppm) 50.72; 51.46; 51.57; 52.95; 55.73; 57.18; 59.26; 123.09; 126.53; 127.11; 141.18; 141.65; 147.42; 150.02; 152.41; 170.48 ESI-MS: $[M+H]^+$ 548.290 (theoretical $[M+H]^+$ 548.294).

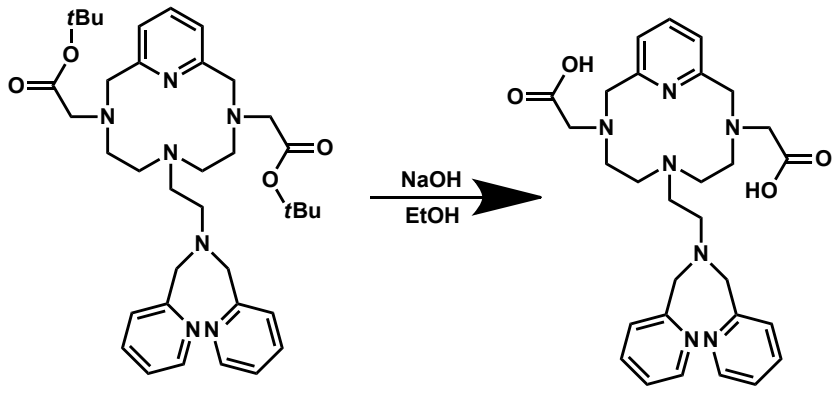

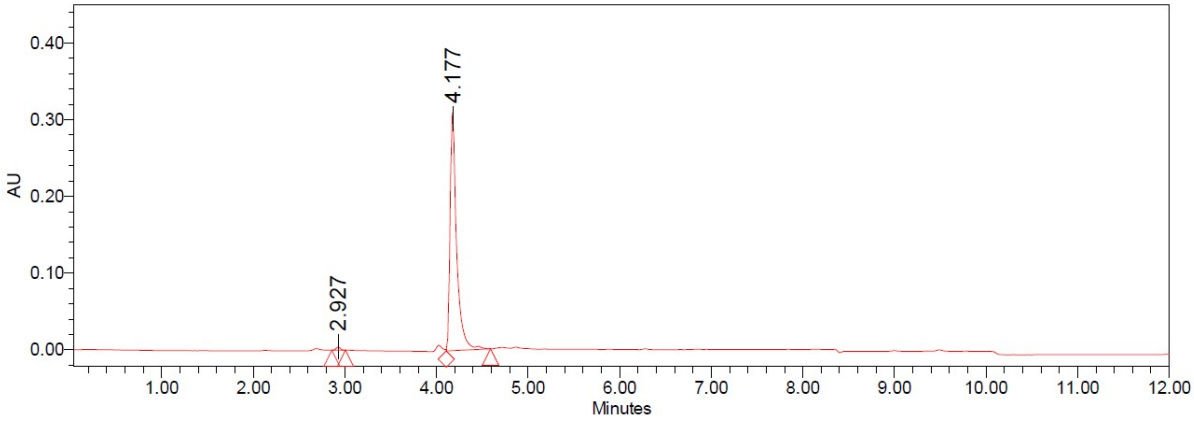

Figure S5. HPLC chromatogram of the product (using the solvent composition as outlined in Table S1, HPLC purity is 99.1%).

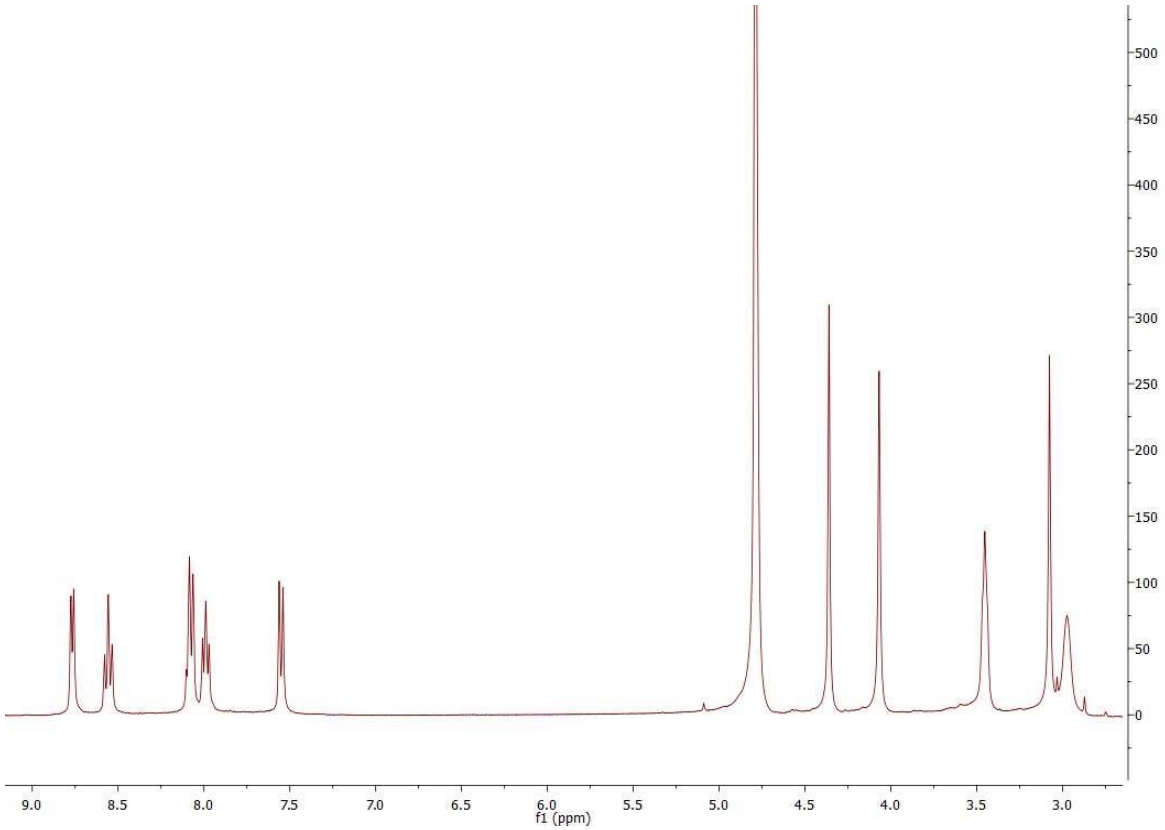

Figure S6. ^{1}H NMR spectrum of the PC2A-DPA ligand (D_2O, 360 MHz, 25 °C at acidic pH).

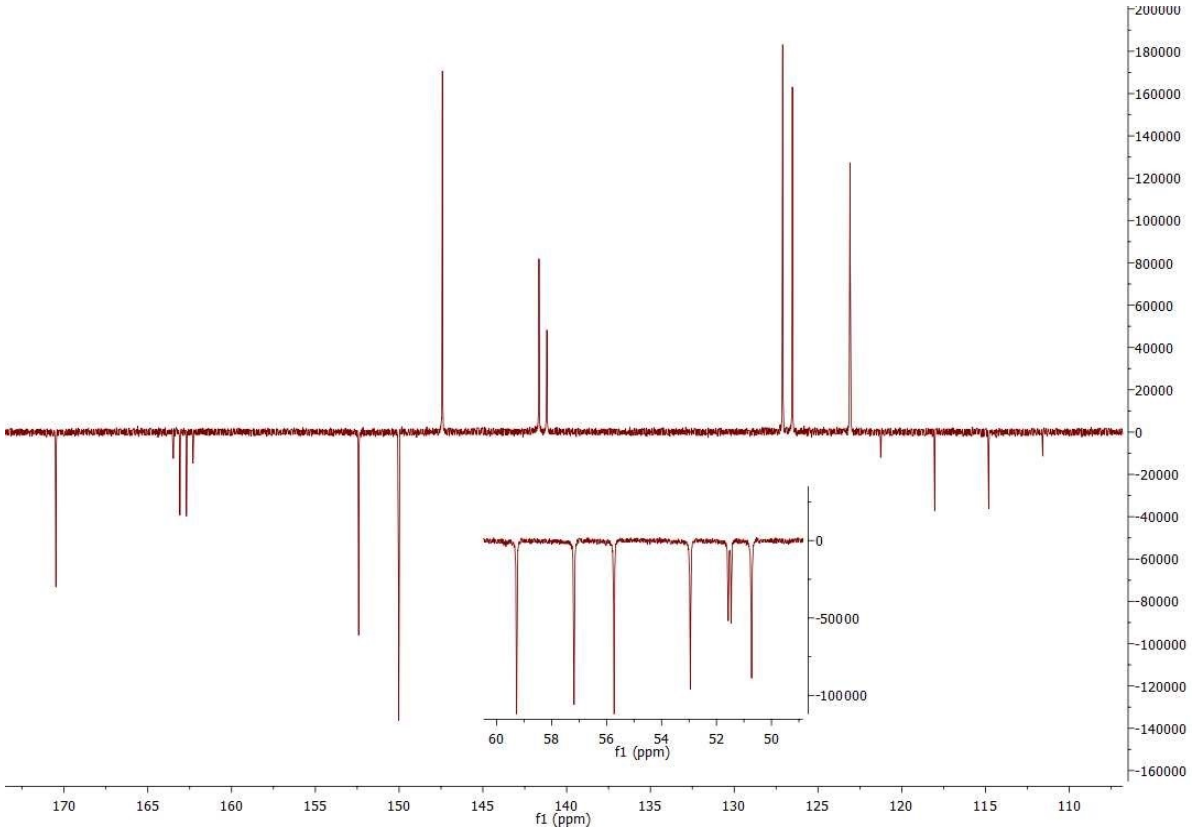

Figure S7. ^{13}C DEPT 135 NMR spectrum of the PC2A-DPA ligand (D_2O, DRX-360 MHz, 25 °C at acidic pH).

Equilibrium studies

The highest analytical grade chemicals were used for the experiments. Complexometric titrations by means of standardized Na_2H_2EDTA solution in the presence of xylenol orange for $ZnCl_2$ and Eriochrome Black T indicator for $MnCl_2$, were carried out to determine the concentration of metal stock solutions.

Methrohm 888 Titrando titration workstation and a *Metrohm-6.0233.100* combined electrode were applied to perform the pH-potentiometric titrations. The electrode was calibrated with two point calibration method using KH-phthalate (pH=4.005) and borax (pH=9.177) as buffers. The titrated samples (6.0 mL) were kept under inert (N_2) atmosphere. During the titration the solutions were stirred and thermostated (25 °C). 0.15 M NaCl was used as ionic strength to mimic the *in vivo* circumstances. The titrations were carried out by using 0.2 M NaOH in solutions containing the ligand or the ligand and metal ions in 1 to 1 and 1 to 2 ratio (c_L=2.00 mM). For the calculation of the protonation and stability constants 100-200 mL–pH data pairs recorded in the pH range of 1.7–12.0, were used. The protonation constants of the ligand (Equation S1) as well as the protonation and stability constants of its metal complexes can be described by the following equations (S2-S6):

$$K_i^H = \frac{[H_iL]}{[H_{i-1}L][H^+]} \qquad i=1\text{-}4 \qquad (1)$$

$$K_{ML} = \frac{[ML]}{[M][L]} \qquad (2)$$

$$K_{ML}^M = \frac{[M_2L]}{[ML][M]} \qquad (3)$$

$$K_{M(H_{i-1}L)}^H = \frac{[M(H_iL)]}{[M(H_{i-1}L)][H^+]} \qquad i=1, 2 \qquad (4)$$

$$K_{M_2L}^{OH} = \frac{[M_2L(OH)][H^+]}{[M_2L]} \qquad (5)$$

$$K_{M_2(OH)L}^{OH} = \frac{[M_2L(OH)_2][H^+]}{[M_2(OH)L]} \qquad (6)$$

For the calculation of $[H^+]$ from the pH values, an 0.01 M HCl solution (0.15 M NaCl) was titrated with known concentrated NaOH solution based on the method proposed by *Irving et al*..[6] The value of K_w (ionic product of water) was calculated from the same titration (pK_w=13.81). PSEQUAD program was used to evaluate the thermodynamic constants.[7]

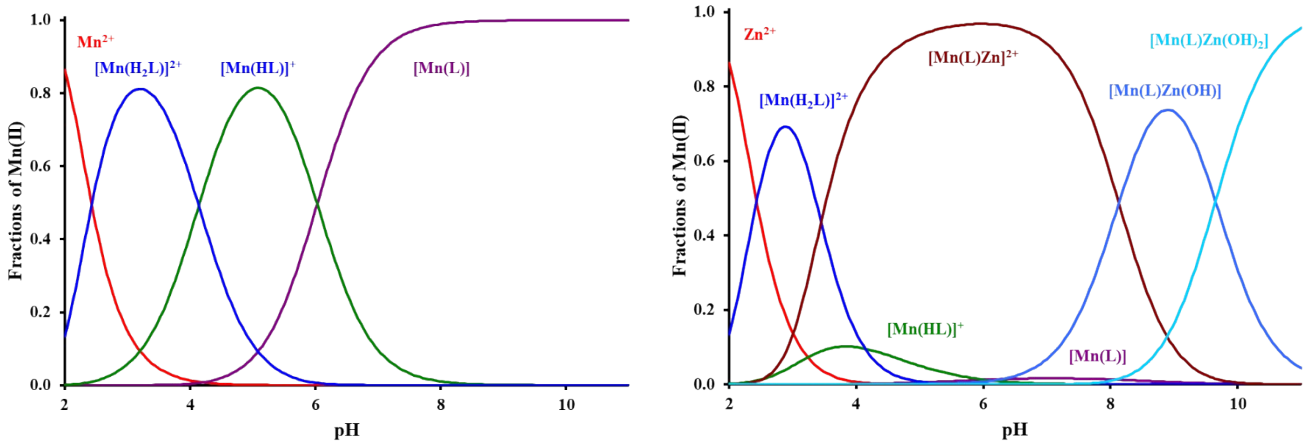

Figure S8. The species distribution curves calculated for the [Mn(PC2A-DPA)(H_2O)] in the absence (left) and in the presence of one equivalent of Zn(II) (right) ($c_{Mn(II)}$=c_{Lig}= $c_{Zn(II)}$=1.0 mM, I=0.15 M NaCl, T=25).

^{1}H-relaxometric studies

The r_{1p} and r_{2p} ($mM^{-1}s^{-1}$) values were measured at 0.49 and 1.41 T field strengths with Bruker Minispec MQ-20 and MQ-60 relaxometers as well as with a Philips Achivea 3 T and a Siemens Magnetom Essenza 1.5 T MR system at 1.5 and 3 T, respectively. The samples were thermostated by using a circulating water bath at 25.0±0.2 and 37.0±0.2 °C. The longitudinal relaxation times (T_1) were measured by the inversion-recovery method (180° − τ − 90°), averaging 5−6 data points for each sample obtained from 10 different τ values. The transversal relaxation times (T_2) were determined by CPMG pulse sequence, again 5-6 identical readouts were averaged. The pH of the samples were maintained by using HEPES buffer (pH=7.40, c_{buffer}=50 mM). The relaxivity data of the complex reported in human serum, lyophilized human or rabbit serum (Seronorm) as well as purified (fatty acid free) human serum albumin (HSA) were prepared by using commercially available substances (Sigma-Aldrich and Sero). Solutions of the [Mn(PC2A-DPA)] or [Mn(PC2A-DPA)Zn_x] complexes (1 mM) were used to dissolve the Seronorm. For determining the affinity constant of the [Mn(PC2A-DPA)Zn]–HSA adduct the method proposed by Terreno and coworkers was used in which the water proton relaxation rates of solutions containing the complex ($c_{[Mn(PC2A-DPA)Zn]2+}$=0.2 mM) and increasing concentrations of the serum protein (c_{HSA}=0.1-2 mM, 8 separated samples) were measured.[8] The pH of the samples was set to pH = 7.4 by using 20 mM HEPES buffer.

Transmetallation of the [Mn(PC2A-DPA)(H_2O)] complex in the presence of Zn^{II} ions

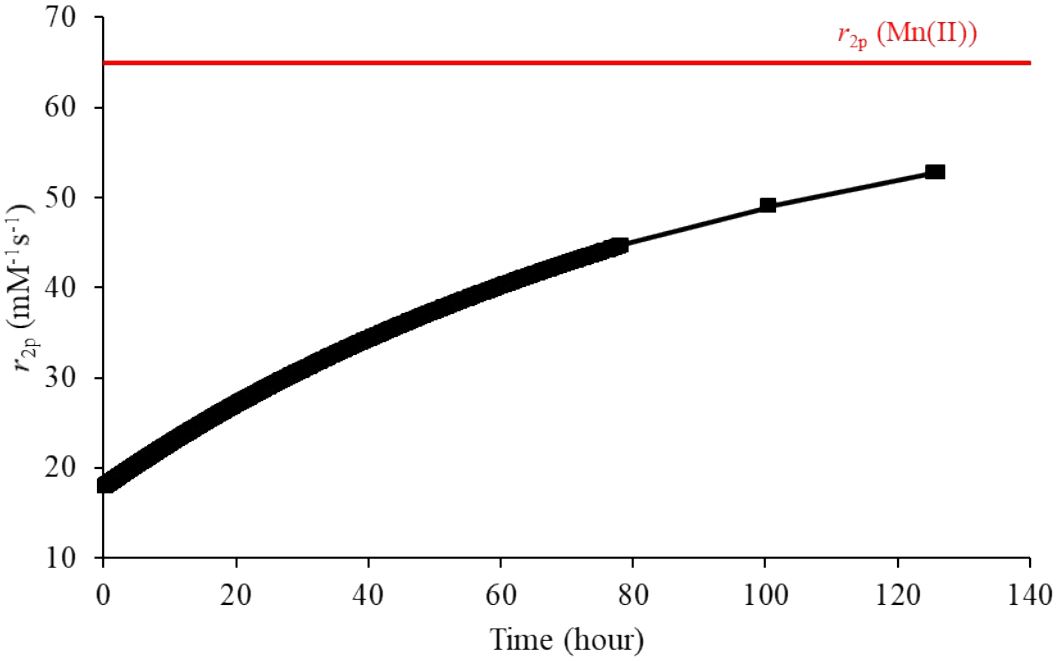

Figure S9. Transmetallation of 1 mM [Mn(PC2A-DPA)] observed in the presence of 25 equivalents of Zn^{II} at pH=6.00 as a function of time, following the conditions proposed by Gale et al. (t= 37 °C and 1.41 T field strength).[9]

HSA affinity of the [Mn(PC2A-DPA)Zn] complex

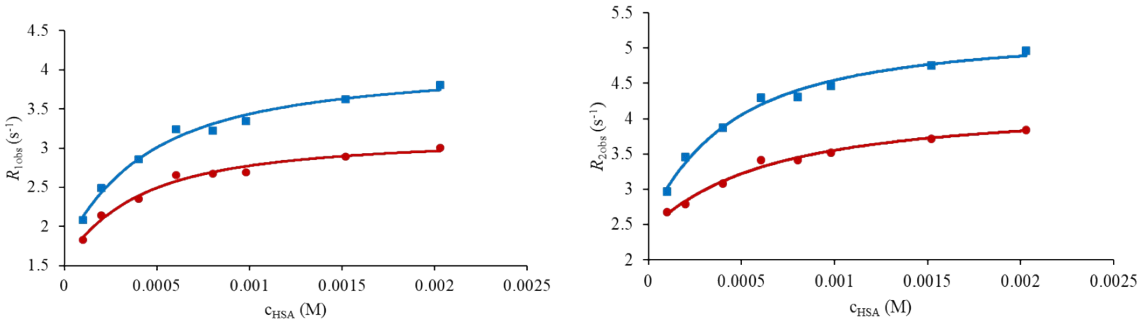

Figure S10. The longitudinal (red) and transvers (blue) relaxation rates of the [Mn(PC2A-DPA)Zn] complex (0.49 T, $c_{complex}$=0.2 mM, pH=7.4) in aqueous solution as a function of increasing HSA concentration at 25 °C (■) and 37 °C (●)

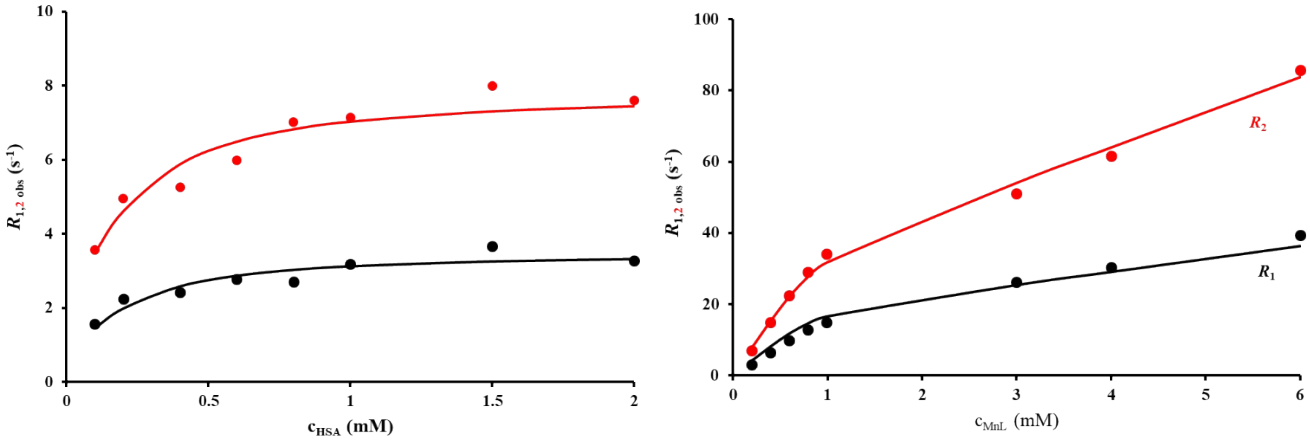

Figure S11. The longitudinal (black) and transvers (red) relaxation rates of the [Mn(PC2A-DPA)Zn] complex ($c_{[Mn(PC2A-DPA)Zn]}$=0.2 mM) as a function of increasing HSA concentration (left) and relaxometric titration of the [Mn(PC2A-DPA)] complex as a function of increasing [Zn(HSA)] concentration ($c_{Zn(II)}$=c_{HSA}=0.8 mM at 37 °C, pH=7.4 and B=1.41 T) (right). Fitting of the data returned the following equilibrium binding constants: 3.9±0.1 and 4.4±0.4.

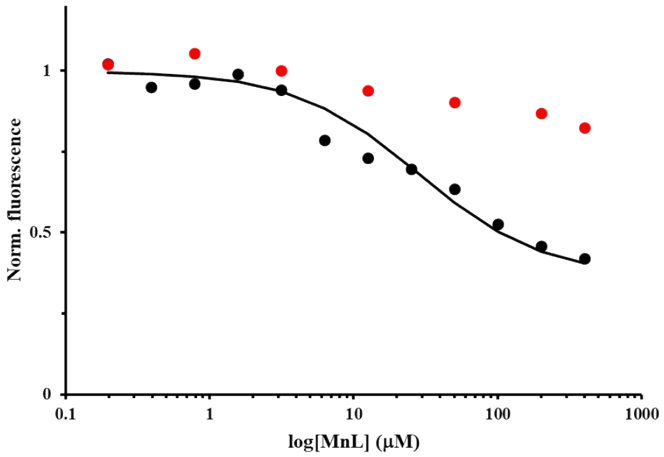

Figure S12. Spectrofluorimetric competition binding curve for the determination of the [Mn(PC2A-DPA)Zn]×[HSA] dissociation constant using dansylglycine (drug site 2 - black) and warfarin (drug site 1 - red) as suggested by A. D. Sherry and co-workers.[10,11]

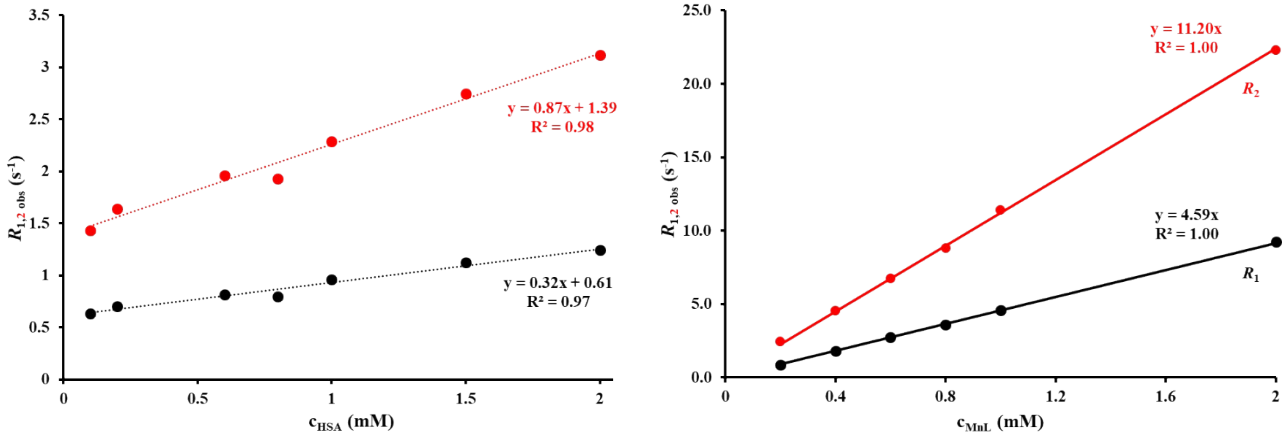

Figure S13. The longitudinal (black) and transvers (red) relaxation rates of the [Mn(PC2A-DPA)] complex (1.41 T, c_{MnL}=0.1 mM, pH=7.4) in aqueous solution as a function of increasing HSA concentration at 37 °C (left) and as a function of [Mn(PC2A-DPA)] concentration (1.41 T, c_{HSA}=0.8 mM, pH=7.4) (right).

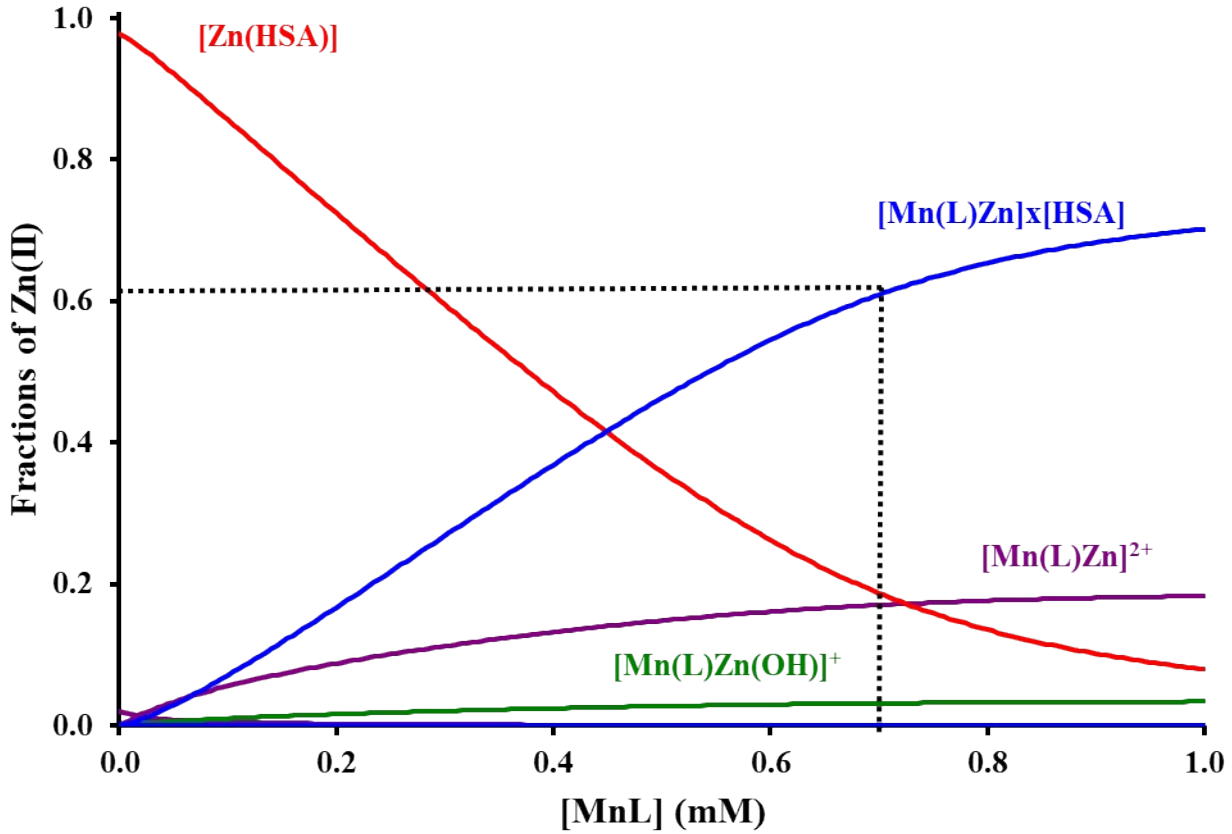

Figure S14. The species distribution curves calculated for the [Mn(PC2A-DPA)Zn]x[HSA] using the stability data shown in Table 1 as well as the conditional binding constant determined in the current study (log K_{aff}=4.4). Conditional binding constant for the [Zn(HSA)] complex is taken form literature[12] ($c_{Zn(II)}$=c_{HSA}=0.7 mM, I=0.15 M, NaCl, T=37 °C).

Table S3. Affinity constants and $r_{(1,2)b}$ ($mM^{-1}s^{-1}$) relaxivities for the formation of the [Mn(PC2A-DPA)Zn]–HSA adduct. The values in **Bold** were evaluated by the simultaneous fitting of the R_{1obs} and R_{2obs} data at a given temperature.

	T_1 measurements		T_2 measurements	
	25 °C	37 °C	25 °C	37 °C
logK_{aff}	3.5±0.2	3.6±0.2	3.5±0.1	3.3±0.1
$r_{(1,2)b}$ ($mM^{-1}s^{-1}$)	20.3±0.8	15.7±0.5	26.2±0.8	20.8±0.7
	25 °C		**37 °C**	
	T_1	T_2	T_1	T_2
logK_{aff}	**3.5±0.1**		**3.5±0.1**	
$r_{(1,2)b}$ ($mM^{-1}s^{-1}$)	**20.0±0.5**	**26.0±0.7**	**16.1±0.5**	**20.0±0.5**

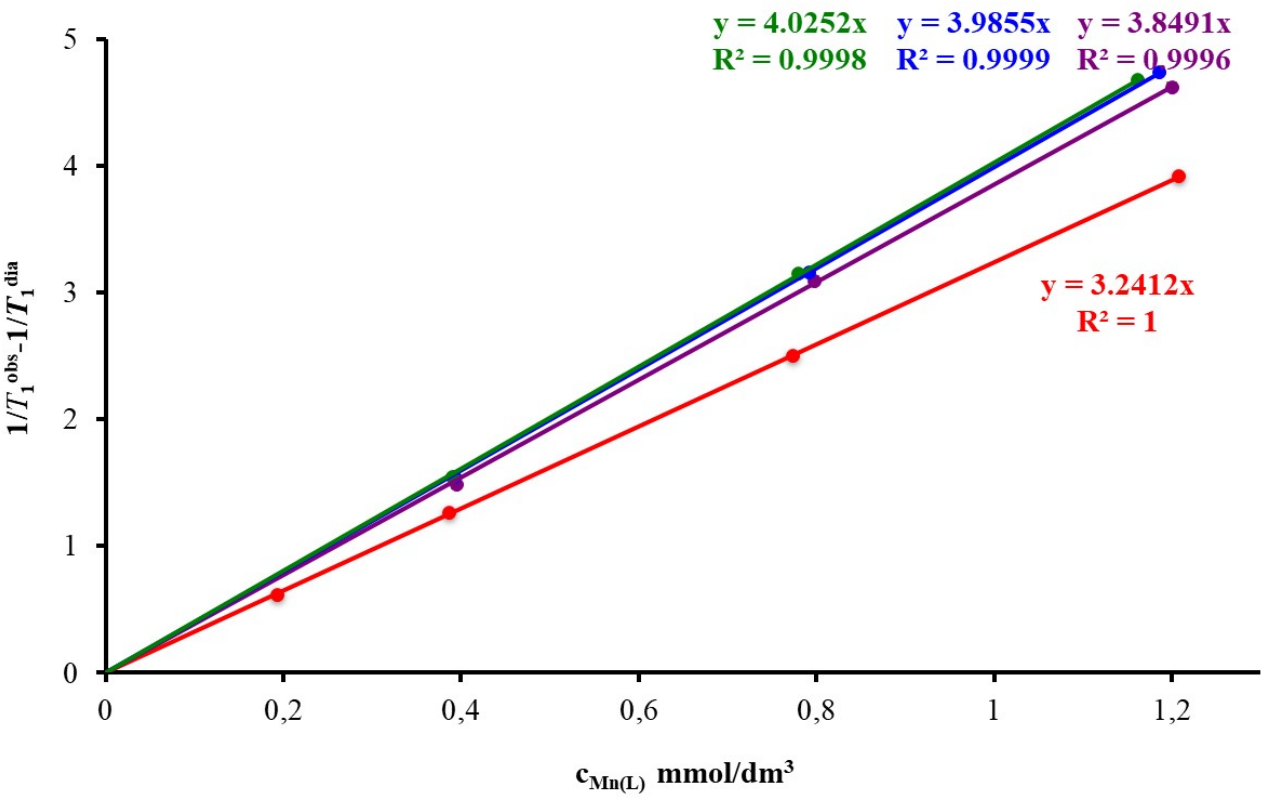

Figure S15. Determination of r_{1p} relaxivity of [Mn(PC2A-DPA)] in the absence and in the presence of half, one and two equivalents of Zn^{II} at 1.41 T and 37 °C (pH=7.4).

Table S4. Relaxation rates observed for the [Mn(PC2A-DPA)] and [Mn(PC2A-DPA)]–Zn adduct in the absence and presence of 0.5, 1 and 2 equivalents of Zn^{II} ions at 1.41 T and 37 °C (pH=7.4)

	r_1 ($mM^{-1}s^{-1}$)	r_2 ($mM^{-1}s^{-1}$)
0.99 mM MnL	3.11	6.89
1.24 mM MnL+0.5 equiv. Zn^{II}	3.99	11.18
0.94 mM MnL+1.0 equiv. Zn^{II}	3.43	9.16
0.92 mM MnL+2.0equiv. Zn^{II}	3.40	9.38
1.12 mM MnL in 0.7 mM HSA	6.83	15.10
0.95 mM MnL+0.5 equiv. Zn^{II} in 0.7 mM HSA	10.27	23.24
0.748 mM MnL+1.0 equiv. Zn^{II} in 0.7 mM HSA	9.08	20.11

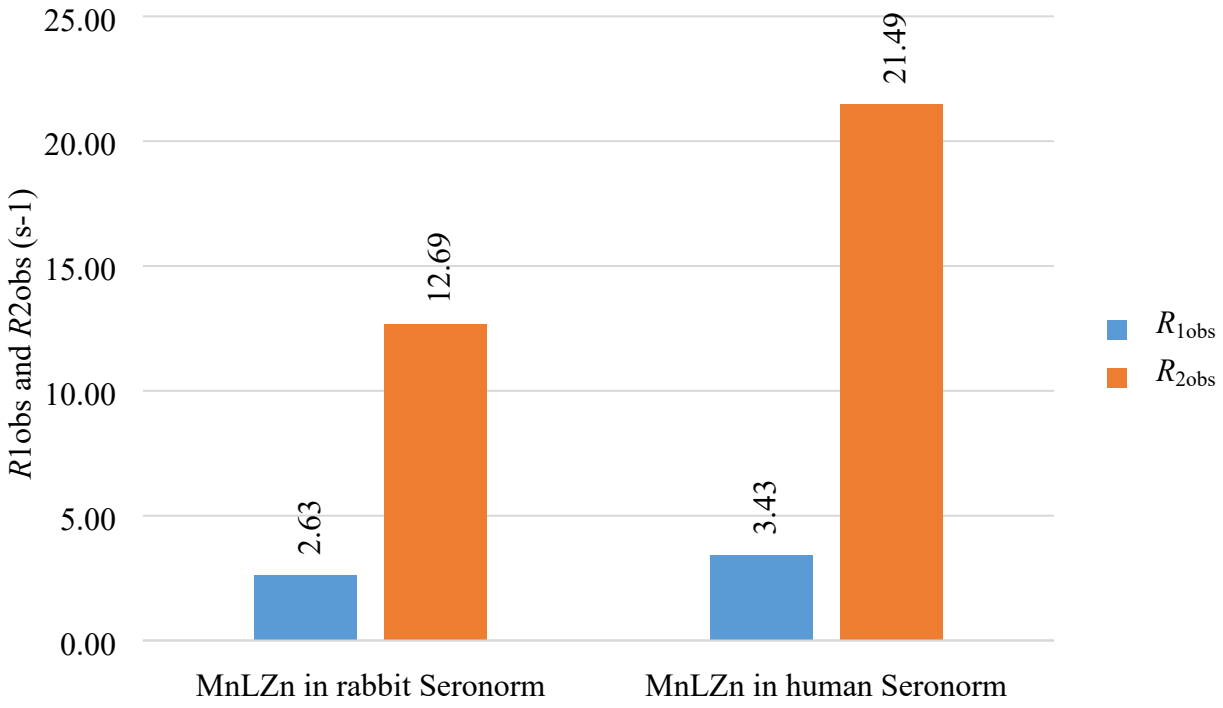

Figure S16. The obtained R_{1obs} and R_{2obs} of [Mn(PC2A-DPA)Zn] complex in rabbit and human Seronorm (3 T, $c_{complexes}$ = 0.2 mM, pH=7.4, 25 °C)

Table S5. Relaxivity values of the [Mn(PC2A-DPA)] and [Mn(PC2A-DPA)Zn] complexes in rabbit serum (Seronorm) (25 and 37 °C, 0.49 and 1.41 T)

	1.41 T, 25 °C		0.49 T, 25 °C	
	r_1 ($mM^{-1}s^{-1}$)	r_2 ($mM^{-1}s^{-1}$)	r_1 ($mM^{-1}s^{-1}$)	r_2 ($mM^{-1}s^{-1}$)
[Mn(PC2A-DPA)]	14.26	39.55	13.74	23.82
[Mn(PC2A-DPA)Zn]	19.58	55.71	22.32	34.33
	1.41 T, 37 °C		0.49 T, 37 °C	
	r_1 ($mM^{-1}s^{-1}$)	r_2 ($mM^{-1}s^{-1}$)	r_1 ($mM^{-1}s^{-1}$)	r_2 ($mM^{-1}s^{-1}$)
[Mn(PC2A-DPA)]	10.17	27.82	11.87	20.06
[Mn(PC2A-DPA)Zn]	16.15	43.42	19.56	29.57

^{17}O NMR measurements

The longitudinal (T_1) and transverse (T_2) relaxation times of the ^{17}O nuclei and its chemical shifts were measured on an aqueous solution of the Mn^{II} complex (pH = 7.4, at 1 mM concentration) and on a diamagnetic reference ($HClO_4$ acidified water, pH = 3.3) in the temperature range 273–348 K using a Bruker Avance 400 (9.4 T, 54.2 MHz) spectrometer. The temperature was determined according to well-established calibration routines using ethylene glycol as standard. T_1 and T_2 values were determined by the inversion−recovery and the CPMG techniques, respectively. To avoid susceptibility corrections of the chemical shifts, a glass sphere fitted into a 10 mm NMR tube was used during the measurements. To increase the sensitivity of ^{17}O NMR measurements, ^{17}O enriched water (10% $H_2{}^{17}O$, NUKEM) was added to the solutions to reach a 2% enrichment. The data fit was carried out with the program Micromath Scientist using least squares fitting procedure. The presence of one water molecule in the inner sphere of the complex was estimated using the method proposed by Gale et al..[13] The reduced water transverse relaxation rates, $\ln(1/T_{2r})$, were fitted to the Swift-Connick equations[11] assuming simple exponential behavior of the electron spin relaxation (Figure S12). The T_1 values and the chemical shifts showed negligible difference between the Mn(II) complex and the reference, thus were not included in the calculations.

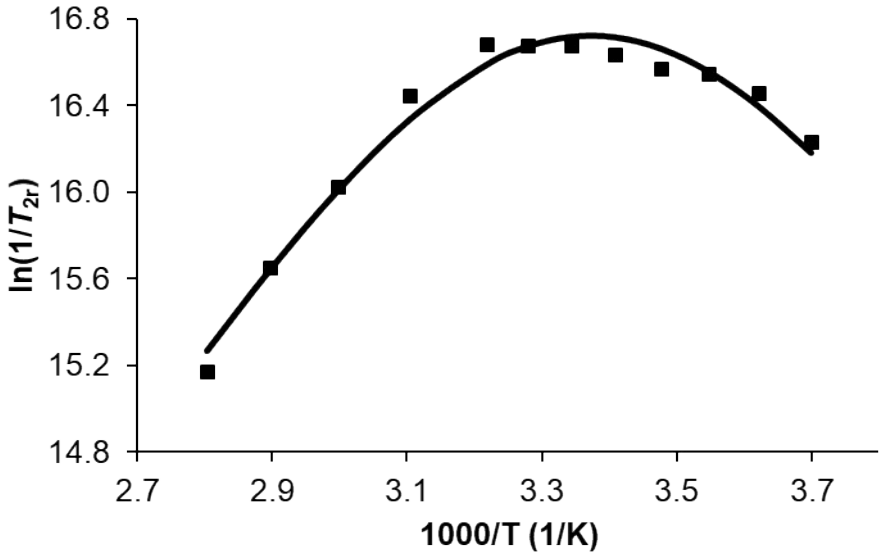

Figure S17. Temperature dependence of the reduced water ^{17}O NMR transverse relaxation rates for [Mn(PC2A-DPA)] at 9.4 T and pH=7.4.

Equation used for the fitting of ^{17}O NMR data

^{17}O NMR data have been fitted according to the Swift and Connick equation.[14] The reduced transverse ^{17}O relaxation rates, $1/T_{2r,}$ have been calculated from the measured relaxation rates $1/T_2$ of the paramagnetic solutions and from the relaxation rates $1/T_{2A}$ of the diamagnetic reference:

$$\frac{1}{T_{2r}} = \frac{1}{P_m}\left[\frac{1}{T_2} - \frac{1}{T_{2A}}\right] = \frac{1}{\tau_m}\frac{T_{2m}^{-2} + \tau_m^{-1}T_{2m}^{-1} + \Delta\omega_m^2}{(\tau_m^{-1} + T_{2m}^{-1})^2 + \Delta\omega_m^2} \tag{S7}$$

$\Delta\omega_m$ is determined by the hyperfine or scalar coupling constant, $A_O/\square$, where B represents the magnetic field, S is the electron spin and g_L is the isotropic Landé g factor (Equation (S08)).

$$\Delta\omega_m = \frac{g_L\mu_B S(S+1)B}{3k_B T}\frac{A_O}{\mathsf{h}} \tag{S8}$$

The ^{17}O transverse relaxation rate is mainly determined by the scalar contribution, $1/T_{2sc}$, and it is given by Equation (S09).

$$\frac{1}{T_{2m}} \cong \frac{1}{T_{2sc}} = \frac{S(S+1)}{3}\left(\frac{A_O}{\mathsf{h}}\right)^2 \tau_s \qquad \frac{1}{\tau_s} = \frac{1}{\tau_m} + \frac{1}{T_1} \tag{S9}$$

The exchange rate, k_{ex}, (or inverse binding time, τ_m) of the inner sphere water molecule is assumed to obey the Eyring equation (Equation (S10)) where $\Delta S^{\ddagger}$ and $\Delta H^{\ddagger}$ are the entropy and enthalpy of activation for the exchange, and $^{298}k_{ex}$ is the exchange rate at 298.15 K.

$$\frac{1}{\tau_m} = k_{ex} = \frac{k_B T}{h}\exp\left\{\frac{\Delta S^{\ddagger}}{R} - \frac{\Delta H^{\ddagger}}{RT}\right\} = \frac{k_{ex}^{298} T}{298.15}\exp\left\{\frac{\Delta H^{\ddagger}}{R}\left(\frac{1}{298.15} - \frac{1}{T}\right)\right\} \tag{S10}$$

For the fit of the ^{17}O T_2 data, we used an exponential function to treat the temperature dependency of $1/T_{1e}$:

$$\frac{1}{T_{1e}} = \frac{1}{T_{1e}^{298}}\exp\left\{\frac{E_v}{R}\left(\frac{1}{T} - \frac{1}{298.15}\right)\right\} \tag{S11}$$

Calculation of the q using the method proposed by Gale et al.[13]

$$q = r_{2\max}^{O}[H_2O]\left(\frac{2}{\sqrt{\frac{S(S+1)}{3}}\frac{A_O}{\mathsf{h}}}\right) \cong \frac{r_{2\max}^{O}}{510} \tag{S12}$$

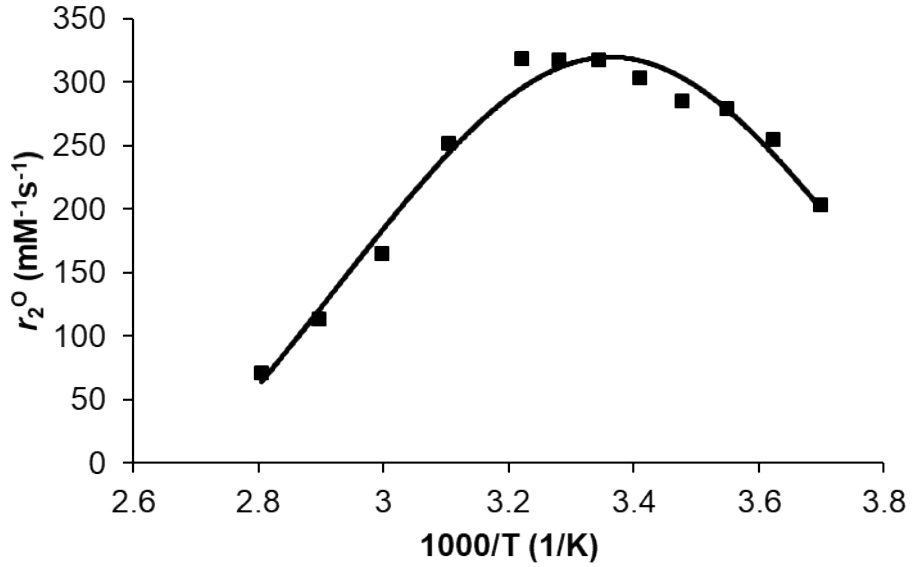

Figure S18. Plots of transverse relaxivity (r_{2max}^{o}) of ^{17}O as a function of temperature for the [Mn(PC2A-DPA)(H_2O)] chelate at 9.4 T (pH=7.4). The solid line represents the Lorentzian fit of the data to determine the maximum value found to be r_{2max}^{o} =318 $mM^{-1}s^{-1}$. The calculated value of the *q* was found to be 0.6±0.2.

In vitro phantom MR imaging

For quantitative MR imaging SIEMENS Magnetom Essenza 1.5 T (system A) and Philips Achivea 3 T (system B) clinical scanners were used. All the MRI scanners were validated. Animal experiments were authorized by the National Scientific Ethical Committee on Animal Experimentation (authorization number # 10/2019/DEMÁB). T_1 values were measured with a series of 2D inversion recovery spin-echo (SE) images of varying inversion times (TIs). The acquisition settings for system A were: TIs =100, 200, 300, 400, 500, 600, 700, 800, 900, 1000, 1200, 1400, 1600, 1800, 2000 msec, repetition times (TRs) = 3630, 3100, 3060, 3130, 3260, 3410, 3580, 3750, 3930, 4110, 4490, 4870, 5260, 5650, 6040 ms, echo time (TE) = 11 msec, acquisition matrix=448x423x20 and image spatial resolution=0.535x0.535x5 mm^3. The settings for system B were: TIs = 200, 300, 400, 600, 800, 1000, 1200, 1400, 1600, 1800, 2000 msec, TR = 3000 ms, echo time (TE) = 15 msec, acquisition matrix=400x226x20 and image spatial resolution=0.449x0.449x4 mm^3. The T_2 values were measured for system A with 2D multiecho SE imaging sequences using TEs = 14.1, 28.2, 42.3, 56.4, 70.5, 84.6, 98.7, 112.8, 126.9, 141.0, 155.1, 169.2, 183.3, 197.4, 211.5, 225.6 msec, repetition time (TR) = 4000 ms, acquisition matrix=384x336x20 and image spatial resolution = 0.573x0.573x3 mm^3. For system B the settings were the followings: TEs = 20, 40, 60, 80, 100 msec, repetition time (TR) = 3000 ms, acquisition matrix=256x201x20 and image spatial resolution = 0.532x0.532x2 mm^3. For each T_1 and T_2 measurement the number of signal averages (NEX) was 1. After defining the volume of interests (VOIs), the MR images were evaluated using MATLAB (MathWorks) software.

The in vivo MRI experiments were approved by the Institutional Animal Care Committee of the University of Debrecen, Hungary (permission number: 10/2019/DEMÁB). Animals involved in the experiments were kept and treated in compliance with all the applicable sections of the Hungarian Laws and directions of the European Union, and the regulations of the Federation of Laboratory Animal Science Associations (FELASA). BALB/c mice (12-week-old, male; n=12) were housed in IVC cages at a temperature of 26±2 °C with 55±10 % humidity and artificial lighting with a circadian cycle of 12 h. Semi-synthetic diet (Akronom Ltd., Budapest, Hungary) and drinking water were available *ad libitum* to all the animals. For the *in vivo* MR imaging studies mice were anaesthetized by 3% isoflurane (Forane) and were injected intravenously with [Mn(PC2A-DPA)] (0.1 mmol/kg body weight) *via* the lateral tail vein with or without intraperitoneal injection of 50 µL 20% (wt/vol) D-glucose. Before (native) and after [Mn(PC2A-DPA)]+glucose injection T_1-weighted (2D axial and 3D GRE EXT multi-FOV; TR/TE 373/4.5 ms; FOV 60 mm; NEX: 4; slice thickness: 1 mm; matrix size: 256x256) and T_2-weighted (2D axial FSE; TR/TE 5132/86.1 ms; FOV 60 mm; NEX: 4; slice thickness: 1 mm; matrix size: 192x256) MRI scans were performed using the preclinical *nanoScan* PET/MRI 3T system (Mediso Ltd., Hungary). MRI images were analyzed using the InterView™ FUSION (Mediso Ltd., Hungary) image analysis

software. Ellipsoidal 3-dimensional Volumes of Interest (VOI) were manually drawn around the edge of the prostate by visual inspection. Experimental data was presented as mean±SD of at least three independent experiments. The significance was calculated by Student's t-test (two-tailed), two-way ANOVA and Mann-Whitney U-test. The significance level was set at $p \leq 0.05$ unless otherwise indicated. In our case (in vivo measurements using the preclinical 3T PET/MR) the scan time for GRE 2D was approximately 6–7 min (1 FOV), and the FSE 2D was approximately 4 min. Each animal was examined 6 times: native T1 and T2 images; images obtained with the use of the probe (T1 and T2) and the probe + glucose addition followed by T1 and T2 imaging. For the in vitro measurements the scan time for T1-weighted and T2-weighted images was approximately 33 min and 18 min at 3T magnetic field, and 47 min and 66 min, respectively at 1.5 T.

Table S6. Quantitative assessment of the relaxation rates (ms) and R_{obs} (s^{-1}, in parenthesis) of the samples by 1.5 and 3 T magnetic field MR imaging ($c_{[Mn(PC2A\text{-}DPA)]}$=0.2 mM, 25 °C, human Seronorm). The values corresponds to the samples presented in the Figure 2. of the main text.

	1.5 T		**3 T**	
samples	T_1**-weighted**	T_2**-weighted**	T_1**-weighted**	T_2**-weighted**
MnLig+HSA	419±7 (2.4)	212±6 (4.7)	543±4 (1.8)	145±5 (6.9)
MnLig	633±9 (1.6)	358±14 (2.8)	693±7 (1.4)	280±9 (3.6)
$MnLigZn_{0.5}$+HSA	304±4 (3.3)	164±3 (6.1)	452±9 (2.2)	102±3 (9.8)
MnLigZn+HSA	275±1 (3.6)	158±3 (6.3)	438±2 (2.3)	89±2 (11.2)
MnLig + Sero	390±3 (2.6)	193±5 (5.2)	519±4 (1.9)	112±3 (8.9)
MnLigZn+Sero	155±3 (6.5)	145±7 (6.9)	292±1 (3.4)	47±1 (21.5)
HSA+buffer	1061±30 (0.94)	515±89 (1.9)	1385±16 (0.7)	717±9 (1.4)

Statistical analysis

Experimental data was presented as mean±SD of at least three independent experiments. The significance was calculated by Student's t-test (two-tailed), two-way ANOVA and Mann-Whitney U-test. The significance level was set at $p \leq 0.05$ unless otherwise indicated.

References

1 N. Lau, J. W. Ziller and A. S. Borovik, Sulfonamido tripods: Tuning redox potentials via ligand modifications, *Polyhedron*, 2015, **85**, 777–782.

2 C. Marín, M. P. Clares, I. Ramírez-Macías, S. Blasco, F. Olmo, C. Soriano, B. Verdejo, M. J. Rosales, D. Gomez-Herrera, E. García-España and M. Sánchez-Moreno, In vitro activity of scorpiand-like

azamacrocycle derivatives in promastigotes and intracellular amastigotes of Leishmania infantum and Leishmania braziliensis, *European Journal of Medicinal Chemistry*, 2013, **62**, 466–477.
3 I. Lázár, Rapid and High Yield Detosylation of Linear and Macrocyclic p-Toluenesulfonamides, *Synthetic Communications*, 1995, **25**, 3181–3185.
4 S. Gabriel, Ueber eine Darstellungsweise primärer Amine aus den entsprechenden Halogenverbindungen, *Ber. Dtsch. Chem. Ges.*, 1887, **20**, 2224–2236.
5 Y. Inoue, M. Taguchi and H. Hashimoto, *N* -Alkylation of Imides with *O* -Alkylisourea under Neutral Conditions, *Synthesis*, 1986, **1986**, 332–334.
6 H. M. Irving, M. G. Miles and L. D. Pettit, A study of some problems in determining the stoicheiometric proton dissociation constants of complexes by potentiometric titrations using a glass electrode, *Analytica Chimica Acta*, 1967, **38**, 475–488.
7 L. Zekany and I. Nagypal, in *Computational Methods for the Determination of Formation Constants*, ed. D. J. Leggett, Springer US, Boston, MA, 1985, pp. 291–353.
8 S. Aime, M. Botta, M. Fasano, S. G. Crich and E. Terreno, Gd(III) complexes as contrast agents for magnetic resonance imaging: a proton relaxation enhancement study of the interaction with human serum albumin, *J Biol Inorg Chem*, 1996, **1**, 312–319.
9 E. M. Gale, I. P. Atanasova, F. Blasi, I. Ay and P. Caravan, A Manganese Alternative to Gadolinium for MRI Contrast, *J. Am. Chem. Soc.*, 2015, **137**, 15548–15557.
10 S. Chirayil, V. C. Jordan, A. F. Martins, N. Paranawithana, S. J. Ratnakar and A. D. Sherry, Manganese(II)-Based Responsive Contrast Agent Detects Glucose-Stimulated Zinc Secretion from the Mouse Pancreas and Prostate by MRI, *Inorg. Chem.*, 2021, **60**, 2168–2177.
11 A. F. Martins, V. Clavijo Jordan, F. Bochner, S. Chirayil, N. Paranawithana, S. Zhang, S.-T. Lo, X. Wen, P. Zhao, M. Neeman and A. D. Sherry, Imaging Insulin Secretion from Mouse Pancreas by MRI Is Improved by Use of a Zinc-Responsive MRI Sensor with Lower Affinity for Zn^{2+} Ions, *J. Am. Chem. Soc.*, 2018, **140**, 17456–17464.
12 E. Ohyoshi, The interaction between human and bovine serum albumin and zinc studied by a competitive spectrophotometry, *Journal of Inorganic Biochemistry*, 1999, **75**, 213–218.
13 E. M. Gale, J. Zhu and P. Caravan, Direct Measurement of the Mn(II) Hydration State in Metal Complexes and Metalloproteins through ^{17}O NMR Line Widths, *J. Am. Chem. Soc.*, 2013, **135**, 18600–18608.
14 T. J. Swift and R. E. Connick, Erratum: NMR-Relaxation Mechanisms of ^{17}O in Aqueous Solutions of Paramagnetic Cations and the Lifetime of Water Molecules in the First Coordination Sphere, *The Journal of Chemical Physics*, 1964, **41**, 2553–2554.